

Review

Controlled Photoradical Polymerization Mediated by 2,2,6,6-Tetramethylpiperidine-1-Oxyl

Eri Yoshida

Department of Environmental and Life Sciences, Toyohashi University of Technology,
1-1 Hibarigaoka, Tempaku-cho, Toyohashi, Aichi 441-8580, Japan; E-Mail: eyoshida@ens.tut.ac.jp;
Tel.: +81-532-44-6814; Fax: +81-532-48-5833

Received: 1 March 2012; in revised form: 13 April 2012 / Accepted: 19 April 2012 /

Published: 2 May 2012

Abstract: In recent years, controlled photoradical polymerization has been established using 2,2,6,6-tetramethylpiperidine-1-oxyl as a mediator. This review article will describe the molecular weight control, polymerization mechanism, influence of initiator structure, effect of substituents supported on photo-acid generator, stability of the propagating chain end, photo-latency of the polymerization, molecular design, and an application to heterogeneous polymerization in an alcoholic medium.

Keywords: controlled photoradical polymerization; 2,2,6,6-tetramethylpiperidine-1-oxyl; azoinitiators; photo-acid generators; methyl methacrylate

1. Introduction

Controlled/living radical polymerizations have made great progress in the past two decades based on their advantages over ionic polymerizations as a simple procedure without severe conditions and widely applicable monomers [1]. Examples of controlled radical polymerizations include: iniferter polymerization [2]; reversible addition fragmentation chain transfer polymerization (RAFT) [3]; atom transfer radical polymerization (ATRP) using transition metal complexes, such as Cu [4], Ni [5], Co [6], Fe [7], Ru [8], Rh [9], Pd [10], and Re [11]; iodide-transfer polymerization [12–14]; and nitroxide-mediated polymerization (NMP) [15,16]. The primary significance of these controlled/living radical polymerizations lies in the fact that the polymerizations can produce precisely designed architectures.

The NMP using 2,2,6,6-tetramethylpiperidine-1-oxyl (TEMPO) has a limited number of

monomers [17–21]; however, the scope of the applicable monomers has been extended by improving the structure of the nitroxide [22–24] using alkoxyamine adducts [25,26] and utilizing additives [27,28]. The NMP still has advantages in using nonmetallic catalysts, thus creating a great variety of architectures through designing the nitroxide catalysts, and producing uncolored or less-colored polymers. While the nitroxides with the 2,2,5-trimethyl-4-phenyl-3-azahexane-3-oxyl skeleton provide highly controlled molecular weight distributions [25], TEMPO also has been often used as the mediator for the NMP, because TEMPO is easily available with a low cost and can be converted into a variety of derivatives that have functional groups [29,30] and are supported on polymers [31–35]. Recent findings that the TEMPO-mediated NMP is induced by photo irradiation involve the significance of the TEMPO mediator [36–51].

Photopolymerization has significant advantages over thermal polymerization in an energy-saving process that utilizes solar energy, local and medical applications, and photo-specific reactions. Hence, considerable attention has been paid to controlled photoradical polymerization to create macromolecules with well-defined structures. For the purpose of establishing controlled photoradical polymerization to well-control the molecular weight, new photoinitiators have been prepared; the dithiocarbamate derivatives [52,53], trithiocarbonate [54,55], dithiodiethanol [56], xanthate [57], and a benzophenone derivative [58]. The potential of photopolymerization has also been explored for thermal RAFT and ATRP polymerizations using photosensitive initiators [59–62] and a catalyst containing dithiocarbamate [63]. More recently, it was found that TEMPO-mediated controlled/living photoradical polymerization provided comparatively narrow molecular weight distribution (MWD) for methyl methacrylate (MMA) [36,37,41,43]. This paper describes TEMPO-mediated controlled/living photoradical polymerization, focusing MMA polymerization and the molecular design through this polymerization.

2. Results and Discussion

2.1. Molecular Weight Control of Polymers

Thermal NMP at high temperatures often causes hydrogen abstraction by the nitroxide mediator from the propagating radical [64,65]. Photopolymerization carried out at room temperature can eliminate this side reaction.

Phtoradical polymerization of MMA was performed by azobis(4-methoxy-2,4-dimethylvaleronitrile) (AMDV) as the initiator and 4-methoxy-TEMPO (MTEMPO) as the mediator in the presence of bis(alkylphenyl)iodonium hexafluorophosphate (BAI) as the photo-acid generator [37]. The bulk polymerization was carried out at room temperature by irradiation with a high-pressure mercury lamp. The orange-colored monomer solution turned colorless after polymerization. These results are shown in Table 1. Polymerization in the absence of MTEMPO produced poly(MMA) (PMMA) with a broad MWD. BAI had a slight effect of decreasing the MWD, although the MWD was still broad. It was found that the MWD dramatically decreased in the presence of MTEMPO.

Table 1. The photoradical polymerization of methyl methacrylate (MMA).

MTEMPO/AMDV	BAI/MTEMPO	Time (h)	Conv. (%)	M_n^a	M_w/M_n^a
– ^b	–	1	85	33,000	6.94
–	– ^c	1	87	32,300	5.86
1.1	–	31	40	11,600	1.47
1.1	0.5	3	68	16,200	1.66
1.1	0.75	2.5	88	19,800	2.88
1.1	1.5	2	95	20,600	3.16
1.4	0.5	9	68	13,600	1.41
2.0	0.5	12	68	10,600	1.55

^a Estimated by GPC based on PMMA standards; ^b [AMDV]₀ = 0.0454 M; ^c [BAI]₀ = 0.0249 M.

Figure 1 shows the GPC profiles of the PMMA obtained in the presence and absence of MTEMPO. The PMMA in the presence of MTEMPO provided a unimodal GPC with a comparatively narrow MWD, whereas the PMMA prepared in its absence showed a bimodal GPC. BAI also affected the MWD in the presence of MTEMPO. As a result of increasing of the molar ratio of BAI to MTEMPO (BAI/MTEMPO), the polymerization was accelerated, so that BAI served as the accelerator of the polymerization. However, the increase in BAI caused the broadening of the MWD of the resulting polymer. On the other hand, an increase in the molar ratio of MTEMPO to AMDV (MTEMPO/AMDV) decelerated the polymerization.

Figure 1. GPC profiles of the poly(MMA) (PMMA) obtained by photoradical polymerization in the (a) absence; and (b) presence of 4-methoxy-TEMPO (MTEMPO).

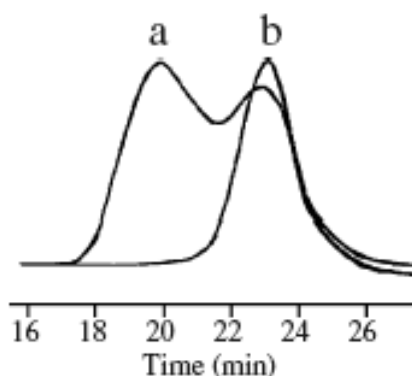


Figure 2 shows the ¹H NMR spectra of BAI, AMDV, and the PMMA ($M_n = 7,030$, $M_w/M_n = 1.60$, conversion = 23%) prepared by the MTEMPO-mediated photopolymerization at MTEMPO/AMDV = 1.1 and BAI/MTEMPO = 0.5. No observed signals originating from BAI in the spectrum of the PMMA indicates that no fragments of BAI were contained in the polymer structure. It is suggested that the BAI fragments did not combine with the growing polymer chain end or MTEMPO, but just interacted with MTEMPO. The polymerization had no effect on the tacticity of PMMA based on the observation of the signals at 0.84 ppm (syndiotactic), 1.01 ppm (atactic), and 1.25 ppm (isotactic) [66]. It was found that the PMMA involved the 1-cyano-1,3-dimethyl-3-methoxybutyl group (CDM) at the chain head and MTEMPO at the chain end. Signals of the methoxy protons originating from CDM were discerned at 3.13–3.22 ppm, while those from MTEMPO were observed at 3.29–3.39 ppm (Figure 3).

The molar ratio of MTEMPO to CDM in the PMMA was estimated to be 0.952 based on their respective methoxy protons, indicating that the PMMA had the CDM and MTEMPO at the 1:1 molar ratio. This good agreement in the molar ratio of MTEMPO/CDM indicates that the growing radical generated by the initiation with the CDM radical was completely captured by MTEMPO (Scheme 1). The molecular weight of the PMMA was estimated by ^1H NMR to be $M_n = 6500$ based on the methoxy protons of CDM and the methyl ester protons of the MMA units. The theoretical molecular weight when the initiator efficiency (IE) determined by UV analysis ($\text{IE} = 0.378$) was taken into account was calculated to be $M_n = 6270$, being in close agreement with the molecular weight estimated by ^1H NMR.

Figure 2. ^1H NMR spectra of the PMMA, bis(alkylphenyl)iodonium hexafluorophosphate (BAI), and azobis(4-methoxy-2,4-dimethylvaleronitrile) (AMDV). Solvent: CDCl_3 .

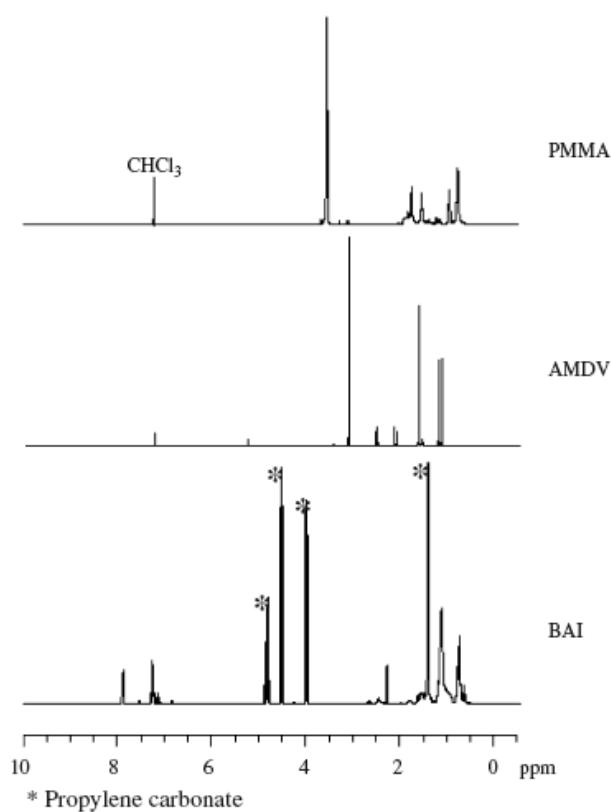
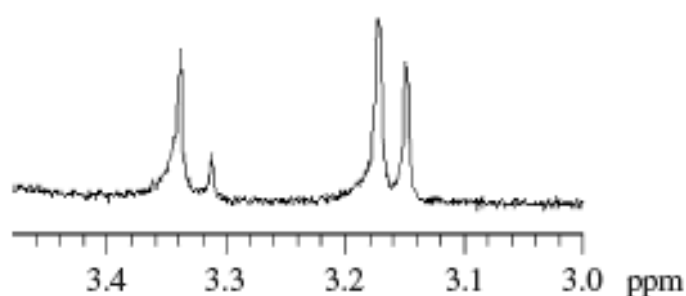
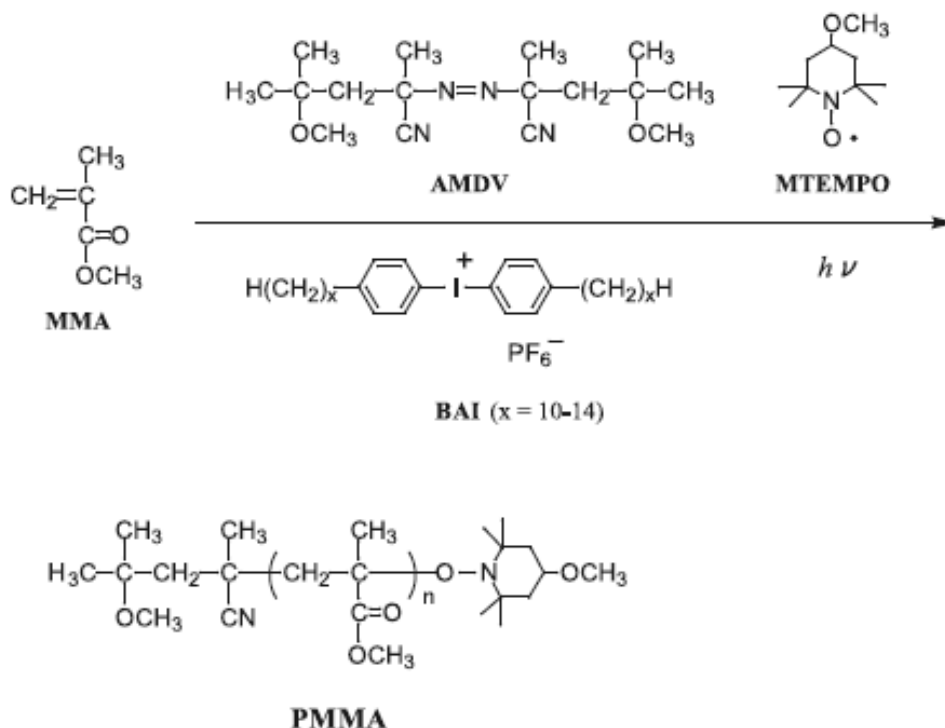


Figure 3. ^1H NMR spectra of the methoxy protons originating from 1-cyano-1,3-dimethyl-3-methoxybutyl group (CDM) and MTEMPO attached to the PMMA chain ends.



Scheme 1. The photoradical polymerization of MMA by AMDV and MTEMPO in the presence of BAI.



The first order time-conversion plots for the polymerization demonstrated that the number of polymer chains was constant throughout the course of the polymerization. The $\ln([M]_0/[M])$ linearly increased over time (Figure 4). As can be seen in Figure 5, the plots of the molecular weight of the resulting PMMA vs. the monomer conversion also linearly increased and the molecular weights were in good agreement with the theoretical molecular weight calculated on the basis on the initiator efficiency ($IE = 0.378$), indicating the livingness of the polymerization. The MWD of the PMMA was maintained at *ca.* 1.6 throughout the polymerization. The GPC curve was shifted to the higher side of the molecular weight with an increase in the conversion (Figure 6), also supporting the living mechanism.

Figure 4. The first order time-conversion plots for the polymerization of MMA. MTEMPO/AMDV = 1.1, BAI/MTEMPO = 0.5. $[M]$ denotes the monomer concentration.

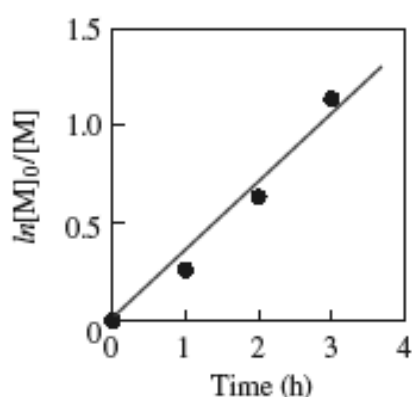


Figure 5. The plots of the molecular weight of the PMMA vs. the conversion. MTEMPO/AMDV = 1.1, BAI/MTEMPO = 0.5.

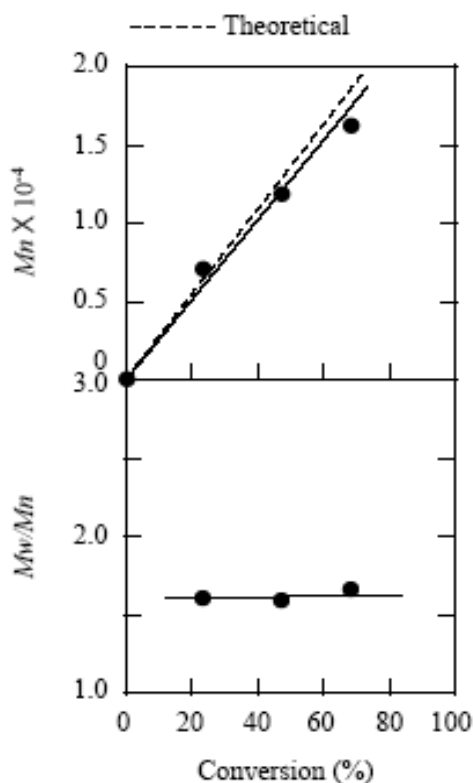
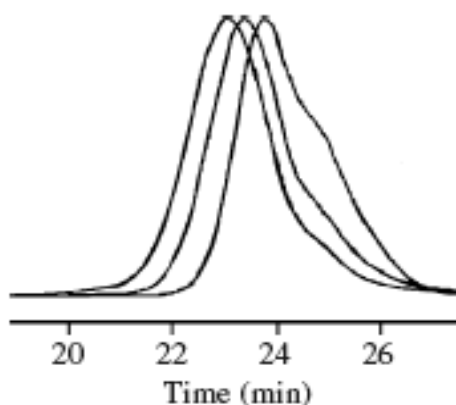
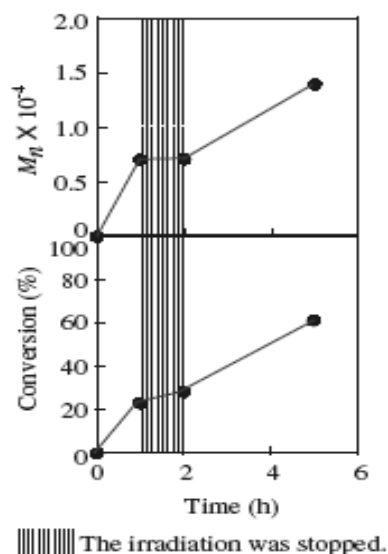


Figure 6. The variation in the GPC curves vs. the conversion: 23% (1 h), 47% (2 h), and 68% (3 h) from the right.



The polymerization was revealed to have a photoswitching ability based on the investigation of the polymerization in the dark. Figure 7 shows the variation in the monomer conversion and molecular weight of PMMA when the irradiation was interrupted for a time during the polymerization. There were negligible changes in the conversion and molecular weight during the dark reaction. However, the conversion and molecular weight increased again by continued irradiation. The progress of the polymerization can be controlled by switching the irradiation on or off.

Figure 7. The variation in the molecular weight of PMMA and conversion when the light was turned off in the middle of the polymerization. MTEMPO/AMDV = 1.1, BAI/MTEMPO = 0.5.



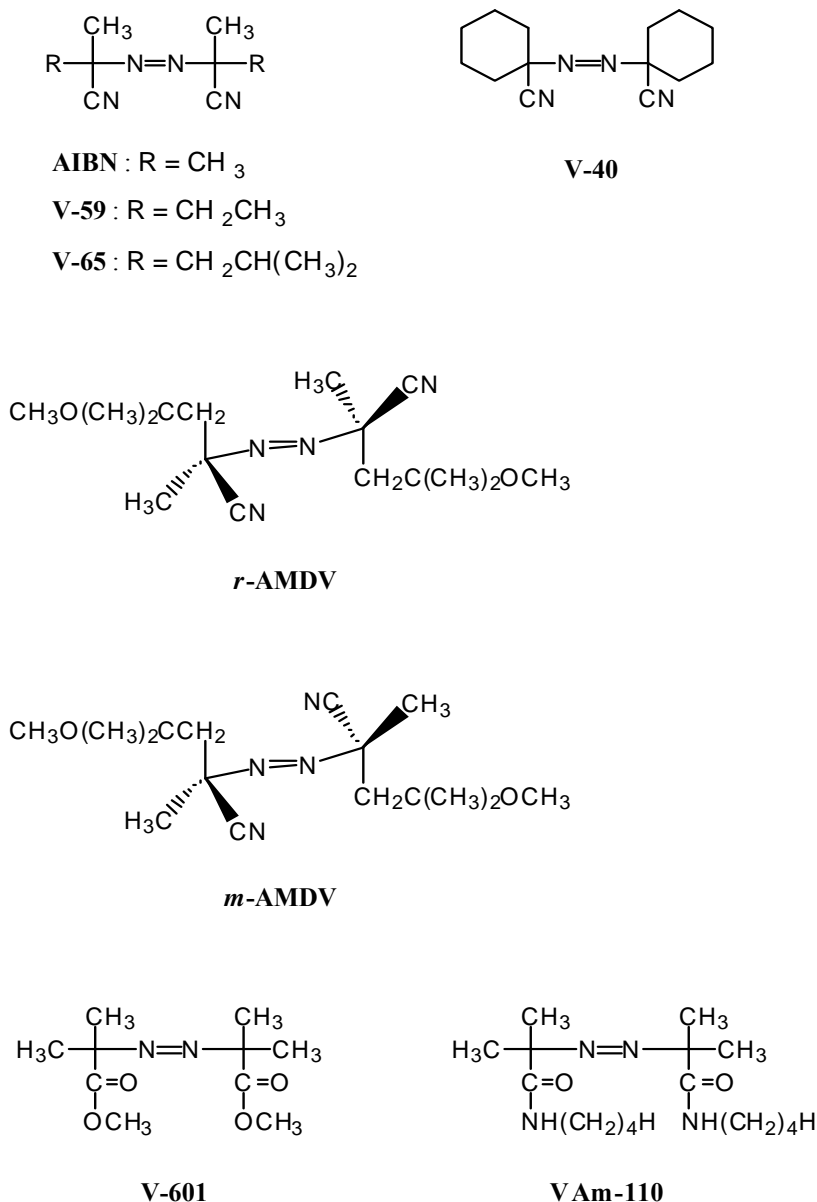
2.2. Effect of Initiators

The MTEMPO-mediated controlled/living photoradical polymerization was performed using the azoinitiator in the presence of the BAI photo-acid generator. In order to clarify which characteristic of the azoinitiator dominates the MWD of the PMMA, the MTEMPO-mediated photopolymerization of MMA was performed using eight different kinds of azoinitiators in the presence of BAI [42]. The azoinitiators are shown in Scheme 2 and the results are summarized in Table 2.

Table 2. The MTEMPO-mediated photopolymerization by the azoinitiators ^a.

Initiators	MTEMPO/Initiator	Conv. (%)	M_n ^b	M_w/M_n ^b	[P] (mM)	IE
AIBN	1	95	39,700	3.37	22.4	0.131
	2	36	15,300	1.68	22.0	0.129
V-59	1	97	31,600	3.37	28.8	0.173
	2	46	15,700	1.66	27.4	0.165
V-65	1	96	18,000	2.33	50.0	0.296
	2	62	9,410	1.53	61.7	0.365
V-40	1	98	38,200	3.24	24.0	0.140
	2	67	26,300	1.65	23.9	0.139
<i>r</i> -AMDV	1	60	7,640	1.52	73.5	0.436
	2	37	3,530	1.28	98.2	0.582
<i>m</i> -AMDV	1	68	10,100	1.50	63.3	0.375
	2	40	4,580	1.34	81.8	0.485
V-601	1	84	26,300	1.99	29.9	0.181
	2	35	10,700	1.68	30.6	0.185
VAm-110	1	25	16,600	1.53	14.1	0.0847

^a [Initiator]₀ = 84.3 mM, BAI/MTEMPO = 0.52. Irradiated for 3 h; ^b Estimated by GPC based on the PMMA standard.

Scheme 2. Azoinitiators used for the MTEMPO-mediated photopolymerization.

The concentration of the growing polymer chain ([P]) was estimated on the basis of the conversion and the molecular weight of the resulting PMMA. Based on the [P], the IE was also determined. Racemic-AMDV (*r*-AMDV), meso-AMDV (*m*-AMDV), V-601, and VAm-110 provided much narrower MWDs with moderate conversions, although VAm-110 produced only a 25% conversion. In particular, *r*-AMDV and *m*-AMDV produced the PMMA with the narrowest MWD. *r*-AMDV had a higher [P] and IE than *m*-AMDV, being in good agreement with the fact that *r*-AMDV has a higher reactivity than *m*-AMDV [67]. As a result of doubling MTEMPO to the initiator, all the initiators produced PMMA with a MWD below 1.7, and the resulting PMMAs showed sharp GPC curves. There were negligible differences in the [P] and IE values between the MTEMPO/initiator ratios of unity and 2.

The characteristics of the UV absorption spectra of the initiators, coupled with their 10-h-half-life temperatures are listed in Table 3. Initiators with higher ϵ values tended to more strictly control the molecular weight and provide a higher IE. The reason that *r*-AMDV, *m*-AMDV, V-601, and

VAm-110 provided much narrower MWDs than the other initiators may partly be due to the fact that these initiators exhibit the $n \rightarrow \sigma^*$ transition in addition to the high ϵ . It was found that the half-lives of the initiators had little effect on the molecular weight control. The [P] and IE were also independent of the half-life temperature.

Table 3. The UV absorption and 10 h half-life temperature of the azoinitiators.

Initiators	λ_{\max} (nm)	Absorbance	ϵ	$T_{1/2}$ (10 h)
AIBN	345	0.176	12.3	65
V-59	348	0.226	15.8	67
V-65	348	0.291	20.4	51
V-40	350	0.236	16.5	88
<i>r</i> -AMDV	348	0.404	28.3	30
	253	0.050	3.50	
<i>m</i> -AMDV	341	0.245	17.2	30
	253	0.078	5.47	
V-601	363	0.273	19.1	66
	253	0.164	11.5	
VAm-110	376	0.455	31.9	110 ^b
	258	2.392	167.7	

2.3. Mechanisms

In order to clarify the mechanism of the MTEMPO-mediated photopolymerization, the polymerization was performed using 1-(cyano-1-methylethoxy)-4-methoxy-2,2,6,6-tetramethylpiperidine (CMTMP), the alkoxyamine adduct as the initiator [39]. CMTMP was prepared by the reaction of MTEMPO and AIBN in methanol. CMTMP had a slight absorption at 257 nm as λ_{\max} ($\epsilon = 3.43$) and almost no overlap with the illumination of the mercury lamp, implying a low photo activity compared to AIBN. The photopolymerization of MMA was performed using CMTMP as the initiator, at room temperature. The results are shown in Table 4.

Table 4. Photo-radical polymerization of MMA by 1-(cyano-1-methylethoxy)-4-methoxy-2,2,6,6-tetramethylpiperidine (CMTMP) in the presence of BAI.

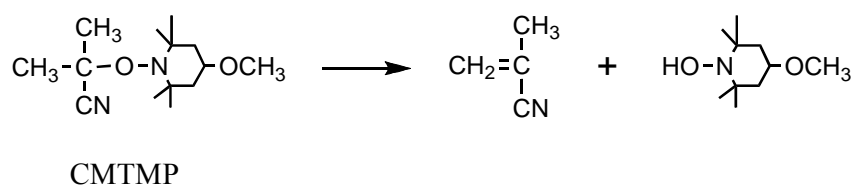
[CMTMP] ₀ (mM)	[BAI] ₀ (mM)	BAI/CMTMP	Time (h)	Conv. (%)	M_n^a	M_w/M_n^a	[P] (mM)	I.E.
47.2	0	0	24	2	—	—	—	—
47.2	5.24	0.11	5	32	27,300	1.68	11.0	0.23
47.2	11.8	0.25	5	51	29,300	1.66	13.7	0.29
47.2	24.9	0.53	5	50	22,600	1.69	17.4	0.37
47.2	47.2	1.0	5	55	16,800	1.78	30.6	0.65
47.2	47.2	1.0	10	94	25,700	2.30	34.2	0.73
31.5	31.5	1.0	11	82	33,400	1.88	23.0	0.73
94.4	94.4	1.0	3.5	92	17,300	2.67	49.8	0.53

^a Estimated by GPC based on the PMMA.

The polymerization only slightly occurred using CMTMP itself; however, it smoothly proceeded in the presence of BAI. The monomer conversion increased with the increasing molar ratio of BAI to

CMTMP (BAI/CMTMP). On the other hand, the molecular weight of the resulting polymer decreased with the increasing BAI/CMTMP ratio, suggesting that the BAI/CMTMP ratio affected the initiator efficiency. The IE of CMTMP was determined on the basis of the concentration of the [P] calculated by the monomer conversion and the molecular weight of the resulting polymer. The IE increased with the increase in the BAI/CMTMP ratio, although it was not quantitative even at 1.0 of BAI/CMTMP. This nonquantitative IE was probably caused by the cage effect and the deactivation of CMTMP by the disproportionation in the hydroxylamine and methyl methacrylonitrile (Scheme 3). In fact, the formation of a significant amount of hydroxylamine lowered the yield of CMTMP in its preparation by the reaction of MTEMPO and AIBN. The molecular weight distributions of the resulting polymers were somewhat broadened as compared to those of the polymers obtained by the photopolymerization by AIBN and 4-methoxy-TEMPO in the presence of BAI [36,67]. This broad molecular weight distribution was probably due to the slow initiation by CMTMP having a low photo activity.

Scheme 3. The disproportionation of CMTMP.



The polymerization was carried out for the different initial concentrations of CMTMP ($[\text{CMTMP}]_0$) at a constant BAI/CMTMP ratio, resulting in the molecular weight of the polymer decreasing with an increase in $[\text{CMTMP}]_0$. The plots of the molecular weight *vs.* the reciprocal of $[\text{CMTMP}]_0$ provided a linear correlation, implying the living nature of the polymerization (Figure 8). Figure 9 shows the GPC profiles of the polymers produced for each conversion. The curves shifted to the higher molecular weight side with an increase in the conversion. The plots of the molecular weight of the polymer *vs.* the conversion are shown in Figure 10. The molecular weight linearly increased with an increase in the conversion; however, the line did not pass through the origin and was almost parallel to the theoretical line. This phenomenon can be accounted for by the fact that a small amount of a polymer with a lower molecular weight was produced during the very early stage before the system reached the steady state of the living polymerization.

Figure 8. The plots of the molecular weight of the resulting polymer *vs.* the reciprocal of $[\text{CMTMP}]_0$. BAI/CMTMP = 1.0.

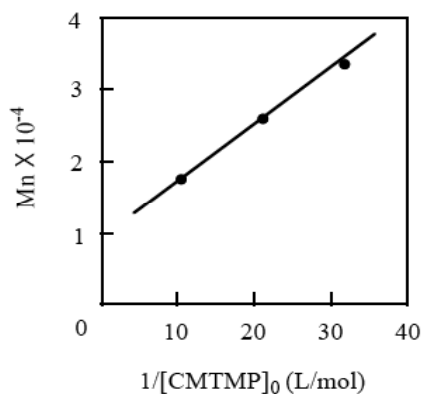


Figure 9. The GPC profiles of the resulting polymer obtained at each conversion: 17% (1 h), 33% (2 h), 48% (3 h), 55% (5 h), 67% (7 h), and 94% (10 h) from the right.

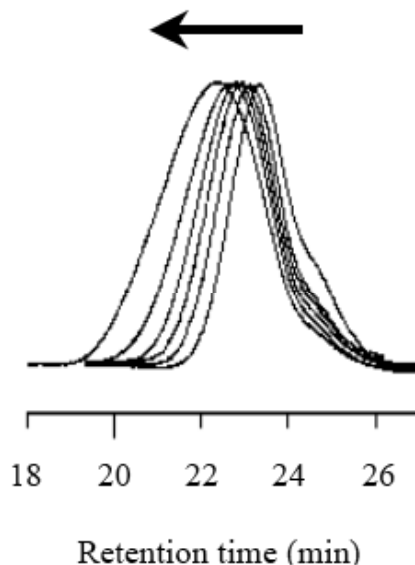
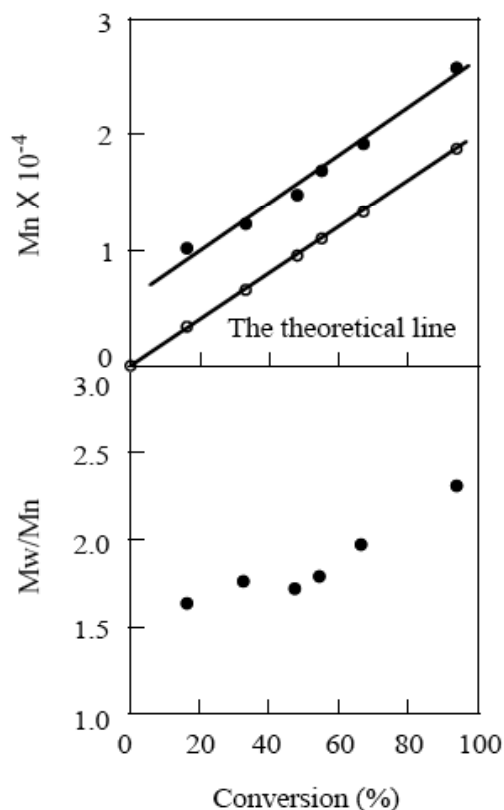


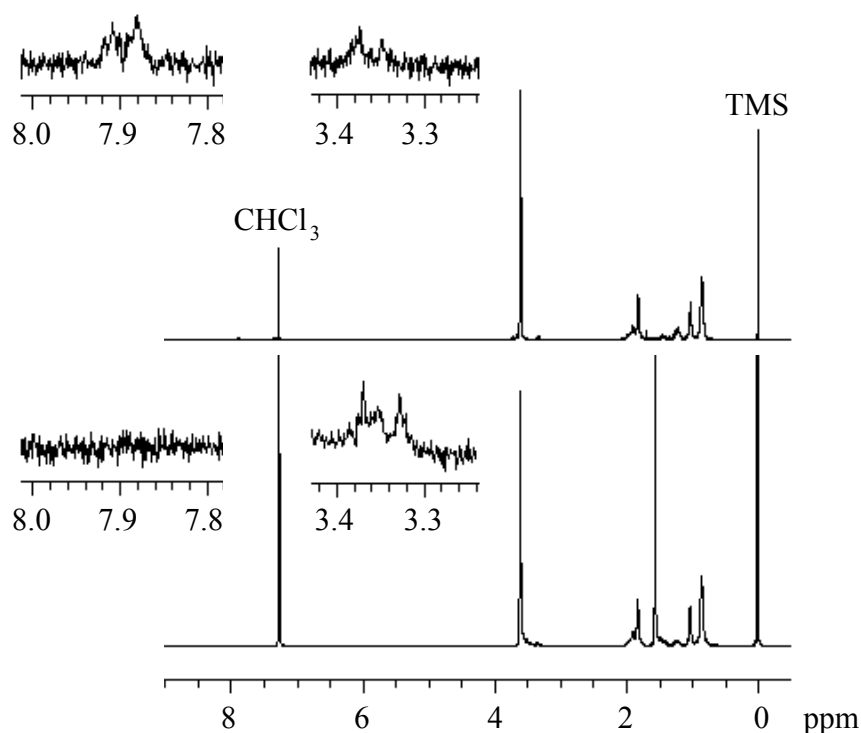
Figure 10. The plots of the molecular weight vs. the conversion. $[CMTMP]_0 = 47.2$ mM, $BAI/CMTMP = 1.0$.



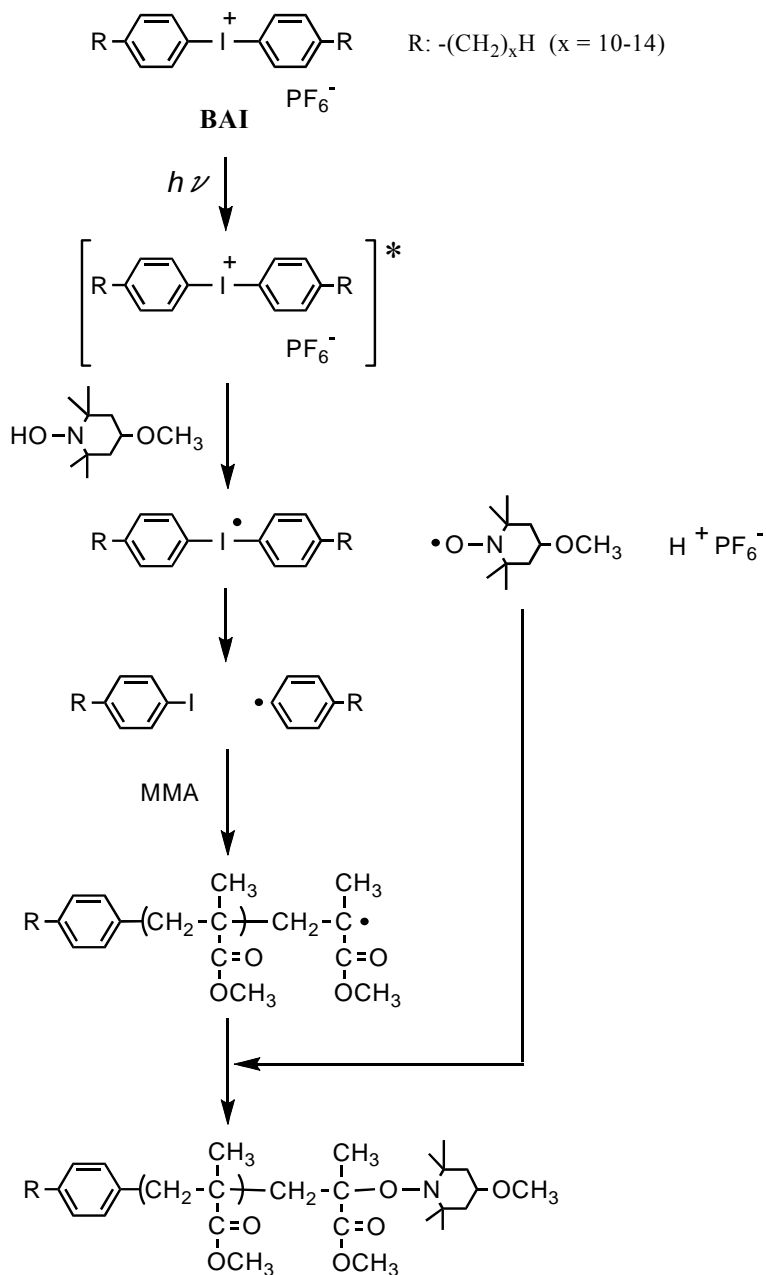
The ^1H NMR analysis revealed that the formation of the polymer, with a low molecular weight during the very early stage before the steady state, was caused by the phenyl radicals generated from CMTMP. Figure 11 shows the ^1H NMR spectra of the polymers obtained by the MTEMPO-mediated polymerization initiated by CMTMP and AIBN/MTEMPO in the presence of BAI. Whereas no BAI

fragments were inserted into the polymer structure prepared from AIBN/MTEMPO, the polymer obtained from CMTMP contained the BAI fragment in its structure, because the aromatic proton signals originating from BAI were discerned at 7.21–7.40 and 7.85–7.92 ppm. The formation of the phenyl radical is supported by the decomposition mechanism of the photo-acid generator [68–70]. The initiation by the phenyl radical was also confirmed by the experiment in which the uncontrolled photopolymerization of MMA performed in the presence of BAI without CMTMP produced a polymer with $M_n = 62,800$ and $M_w/M_n = 3.77$ at 84% conversion within only 2 h. During the MTEMPO-mediated polymerization, the propagating chains formed by the phenyl radical probably participated in the controlled polymerization by MTEMPO by obtaining the counter radical from the hydroxylamine (Scheme 4) because the GPC curves were shifted to the higher molecular weight side without deactivation with the increasing conversion. In the MTEMPO/AIBN system, the propagation proceeded by repeating the dissociation and recombination of the C-ON bond, as well as the thermal polymerization, since no BAI fragments were contained in the polymer structure. However, electron transfer is expected to occur between MTEMPO and BAI in the excited state during the dissociation and recombination when it is taken into consideration that continued polymerization is difficult in the absence of BAI and that the excited diphenyliodonium salt easily receives an electron [68–70]. Consequently, the mechanism of the polymerization was thus proposed (Scheme 5).

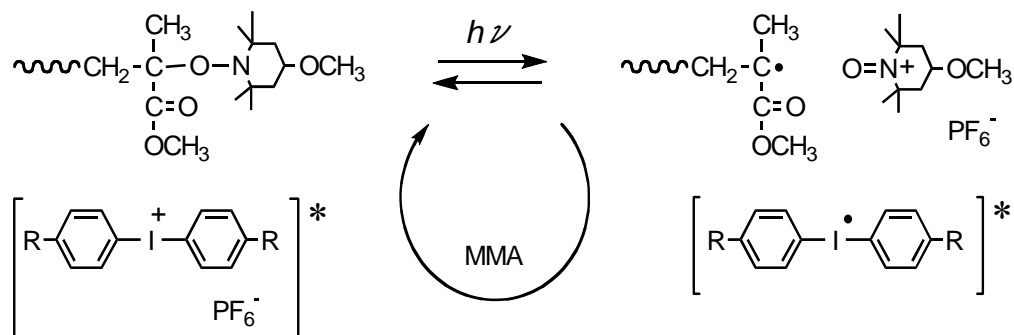
Figure 11. The ^1H NMR spectra of the polymers obtained by the MTEMPO-mediated polymerizations initiated by CMTMP (**upper**, $M_n = 10,195$ and $M_w/M_n = 1.63$) and AIBN (**lower**, $M_n = 9,140$ and $M_w/M_n = 1.57$) in the presence of BAI. Solvent: CDCl_3 .



Scheme 4. The initiation by the phenyl radical.



Scheme 5. The propagation mechanism.



2.4. Effects of Photo-Acid Generators

2.4.1. Triarylsulfonium Salts

Triarylsulfonium salts are known as efficient photoinitiators for cationic polymerization as are diaryliodonium salts. While triarylsulfonium salts show a lower photosensitivity than the diaryliodonium salts [68,71], the sulfonium salts have advantages over the diaryliodonium salts in the extraordinary thermal stability [72] and easier preparation [73]. In order to precisely control the molecular weight of polymers, the MTEMPO-mediated photopolymerization was performed using the triarylsulfonium salt instead of the diaryliodonium salt.

The polymerization of MMA was performed at room temperature using (4-*tert*-butylphenyl)diphenylsulfonium triflate (^tBuS) as the photo-acid generator by the *r*-AMDV initiator and the MTEMPO mediator [41]. The results are shown in Table 5. While the polymerization slowly occurred in the absence of ^tBuS, the polymerization smoothly proceeded in its presence. The ^tBuS/MTEMPO molar ratio increased [P], resulting in a decrease in the molecular weight of the resulting polymer. There was a tendency that the polymerization was accelerated as the ^tBuS/MTEMPO ratio increased. The polymerization rate was also dependent on MTEMPO because the large excess of MTEMPO to *r*-AMDV retarded the polymerization even in the presence of ^tBuS. The MWD was significantly broadened at a MTEMPO/*r*-AMDV less than 1, suggesting less control of the polymerization. Furthermore, no polymerization occurred in the absence of *r*-AMDV, although ^tBuS solely initiated the polymerization to produce a polymer with a very broad MWD. It is implied that MTEMPO controlled the polymerization.

Table 5. Photoradical polymerization of MMA by MTEMPO and ^tBuS ^a.

[MTEMPO] ₀ (mM)	[^t BuS] ₀ (mM)	MTEMPO/ AMDV	^t BuS/MTEMPO	Time (h)	Conv. (%)	M _n ^b	M _w /M _n ^b	[P] (mM)
48.3	–	1.06	–	31	40	11,600	1.47	32.3
48.3	12.8	1.06	0.265	9	63	13,200	1.46	44.8
48.3	23.5	1.06	0.487	9	63	11,100	1.46	53.0
48.3	34.1	1.06	0.706	9	64	10,200	1.44	59.0
48.3	47.0	1.06	0.973	6	77	15,700	1.58	46.0
48.3	70.4	1.06	1.46	6	71	11,100	1.45	60.1
80.5	66.2	1.77	0.822	23	74	9,350	1.51	74.1
91.3	91.8	2.01	1.01	23	82	7,790	1.70	98.5
91.3	47.0	2.01	0.515	14	26	4,670	1.36	52.1
21.5	10.7	0.473	0.498	5	71	18,300	1.76	36.4
48.3	25.6	– ^c	0.530	6	0	–	–	–
–	94.4	– ^c	–	3	73	417,000	19.6	1.64

^a [AMDV]₀ = 45.4 mM; ^b Estimated by GPC based on the PMMA standard; ^c Without AMDV.

The livingness of the polymerization was evaluated at the MTEMPO/*r*-AMDV of 1.06 and ^tBuS/MTEMPO of 0.487. The first order time-conversion plots for the polymerization are shown in Figure 12. The $\ln([M]_0/[M]_t)$ almost linearly increased with time, suggesting that the number of polymer chains was constant throughout the course of the polymerization. Figure 13 shows the plots of

the molecular weight, MWD, and $[P]$ vs. the conversion. The molecular weight linearly increased with the increasing conversion and was in a good agreement with the theoretical values. The MWD remained constant at around 1.45. The $[P]$ also remained at *ca.* 45 mM, indicating the constant number of polymer chains. The GPC profiles of the resulting polymer for each conversion are shown in Figure 14. The curves were shifted to the higher molecular weight side with the increasing conversion. Based on the GPC analysis, coupled with the linear correlations of the first order time-conversion and conversion-molecular weight plots, it can be deduced that the polymerization proceeded by a living mechanism and that t BuS more effectively controlled the molecular weight than BAI.

Figure 12. The first order time-conversion plots for the polymerization of MMA. MTEMPO/*r*-AMDV = 1.06, t BuS/MTEMPO = 0.487.

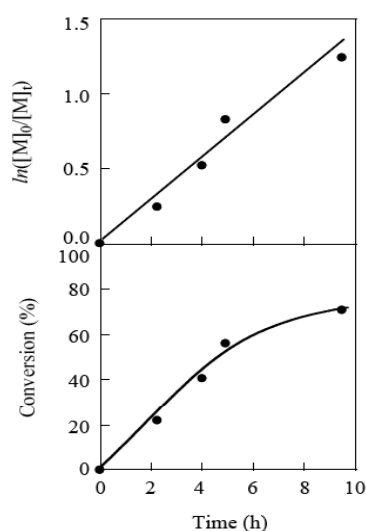


Figure 13. The plots of the molecular weight, molecular weight distribution, and $[P]$ vs. the conversion. MTEMPO/*r*-AMDV = 1.06, t BuS/MTEMPO = 0.487.

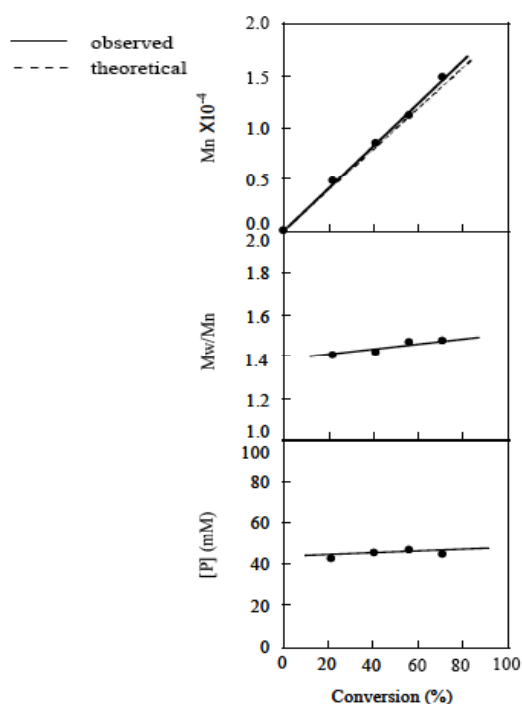
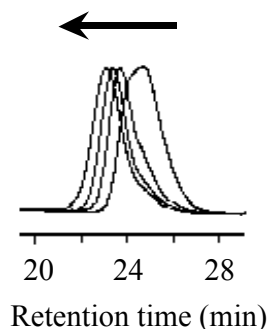
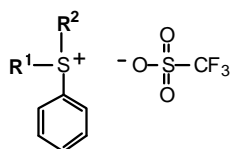


Figure 14. GPC profiles of the PMMA obtained at each conversion: 22% (2.25 h), 41% (4.00 h), 56% (4.92 h), and 71% (9.50 h) from the right.



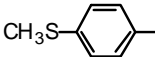
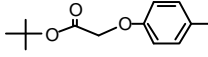
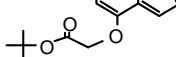
In order to explore the influence of the substituents attached to the sulfonium salt on the polymerization, the polymerization was performed using 13 different sulfonium salts [43]. These results are shown in Table 6. The solubility of the sulfonium salt in MMA had no influence on the MWD, because the heterogeneous solution including the insoluble sulfonium salt became homogeneous within 1 h of the irradiation. There was a negligible difference in [P] and IE, independent of the substituents. The substituents produced a significant difference in the MWD. The sulfonium salts with the alkyl, methoxy, phenoxy, methylthio, and *tert*-butoxycarbonylmethoxy groups had no effect on the molecular weight control because the MWDs of the polymers obtained by these sulfonium salts were close to that by the triphenylsulfonium triflate (Run 1). Halogens with the exception of the iodide also had a negligible effect on it. These polymers had similar GPC profiles. On the other hand, the iodide, phenylthio, and naphthyl groups on the sulfonium salts caused broad MWDs with the bimodal GPCs including a peak on the higher molecular weight side. These functional groups should have competitively participated in the electron transfer between the sulfonium salt and MTEMPO during the propagation, resulting in the formation of polymers with uncontrolled high molecular weights.

Table 6. The MTEMPO-mediated photopolymerization of MMA in the presence of the sulfonium salts ^a.



Run no.	R ¹	R ²	Solubility ^b	Conv. (%)	M _n ^c	M _w /M _n ^c	[P] (mM)	IE
1			I	63	12,200	1.42	48.2	0.531
2			S	52	10,200	1.39	47.8	0.527
3			S	58	11,000	1.43	49.5	0.545
4			I	62	11,000	1.50	52.9	0.582
5			S	46	9,810	1.45	43.9	0.483
6			S	80	427,000 ^d 14,000	3.64 1.70	40.1	0.442

Table 6. Cont.

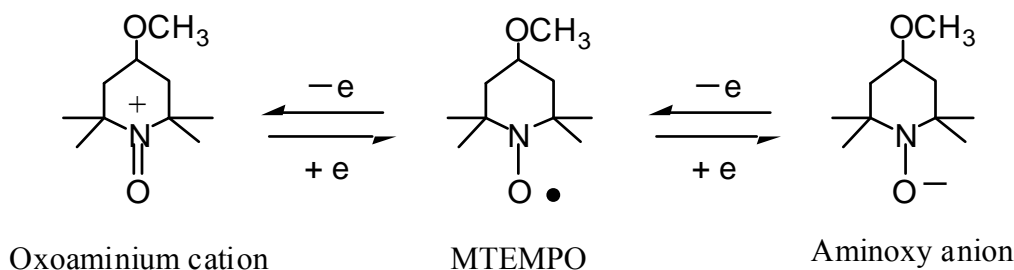
Run no.	R ¹	R ²	Solubility ^b	Conv. (%)	M _n ^c	M _w /M _n ^c	[P] (mM)	IE
7		CH ₃ —	S	66	12,200	1.45	51.0	0.562
8			S	58	12,600	1.44	43.0	0.474
9			S	64	11,400	1.45	52.3	0.577
10			I	53	11,000	1.44	45.0	0.496
11			S	70	12,100	1.49	54.0	0.594
12			I	62	10,100	3.14	57.5	0.634
13			I	73	13,200	2.40	51.9	0.571

^a MTEMPO/*r*-AMDV = 1.1, Sulfonium salt/MTEMPO = 0.5. Irradiated for 6 h; ^b Solubility of the sulfonium salts. S: Soluble, I: Insoluble; ^c Estimated by GPC based on the PMMA standard; ^d Bimodal GPC. The area ratio: Mn(427,000/14,000) = 0.26/0.74.

2.4.2. An Iron-Arene Complex

Iron-arene complexes act as photoinitiators for cationic polymerizations as well as diaryliodonium salts and triarylsulfonium salts. For the MTEMPO-mediated polymerization, the diaryliodonium salts and triarylsulfonium salts did not directly engage in controlling the growing polymer radicals, but enhanced the polymerization rate by interacting with MTEMPO accompanied by the growing polymer radical. It was considered that the interaction was attributed to the electron transfer between these onium salts and MTEMPO in their excited states. This electron transfer mechanism was based on the fact that MTEMPO forms the redox systems in which MTEMPO is converted into the oxoammonium cation by the one-electron oxidation, while it is converted into the aminoxy anion by the one-electron reduction (Scheme 6) [74].

Scheme 6. The redox systems of MTEMPO.



The iron-arene complexes are more stable toward the electron transfer due to the redox formation of the iron than the iodonium salts and sulfonium salts [75]. The MTEMPO-mediated photopolymerization of MMA was performed using (η^6 -benzene)(η^5 -cyclopentadienyl)Fe^{II} hexafluorophosphate (BzCpFe^{II}) as the accelerator (Table 7) [46]. The conversion reached 73% at 3 h, however, it did not increase over this time. It is likely that the conversion reached its plateau at 3 h. It was found that an increase in the

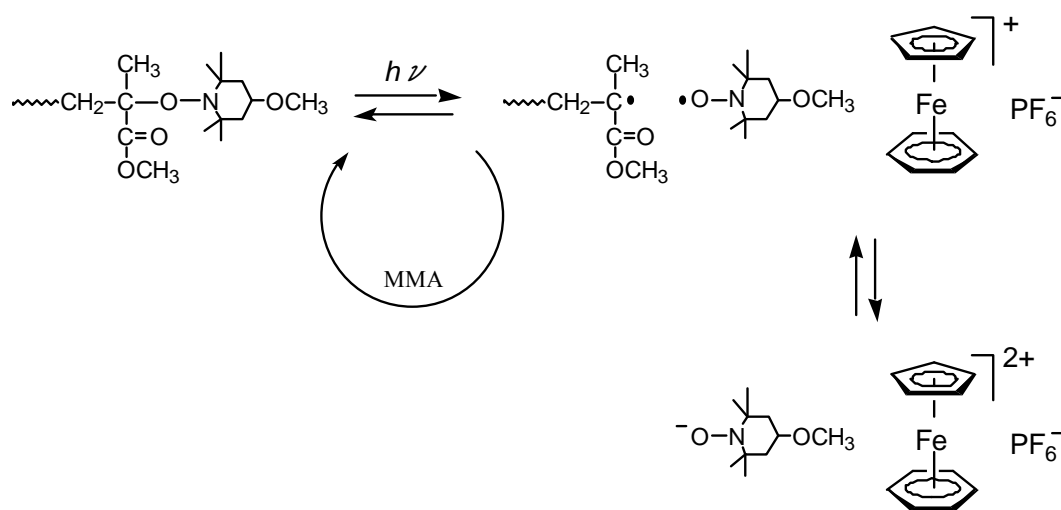
amount of BzCpFe^{II} retarded the polymerization rate. BzCpFe^{II} showed the opposite tendency against BAI and ^tBuS that enhanced the polymerization rate [36,37,41]. It is suggested that BzCpFe^{II} is different from the diaryliodonium salts and triarylsulfonium salts regarding the molecular weight control mechanism. For the BzCpFe^{II} redox system, the reduction redox system between MTEMPO and the aminoxy anion is involved in the electron transfer interaction, while the oxidation redox system between MTEMPO and the oxoammonium cation is used for the onium salt redox systems (Scheme 7). The polymerization using BzCpFe^{II} also proceeded by a living mechanism, since the first-order time-conversion plots and conversion-molecular weight plots showed linear increases. The MWDs retained Mw/Mn = 1.4–1.5 during the polymerization.

Table 7. The MTEMPO-mediated photopolymerization of MMA in the presence of BzCpFe^{II}.

<i>r</i> -AMDV (μmol)	MTEMPO (μmol)	BzCpFe ^{II} (μmol)	Time (h)	Conv. (%)	<i>Mn</i> ^a	<i>Mw/Mn</i> ^a
45.4	48.3	48.3	3	73	17,500	1.54
45.4	48.3	48.3	4	66	16,700	1.58
45.4	48.3	96.5	7	46	11,500	1.47
–	–	48.3	3	6	90,500	3.09
–	48.3	48.3	3	20	48,300	2.45
45.4	–	48.3	1	80	15,100	7.21

^a Estimated by GPC based on PMMA standards.

Scheme 7. The electron transfer between MTEMPO and BzCpFe^{II}.



2.5. Stability of the Growing Polymer Chain End

The thermal NMP is often deactivated through the hydrogen elimination from the growing polymer radical by the nitroxide at the end stage of the polymerization [64,76,77]. The stability of the growing polymer chain ends for the MTEMPO-mediated photopolymerization of MMA was investigated by the block copolymerization with isopropyl methacrylate (ⁱPMA) [44]. The block copolymerization of ⁱPMA was performed using the PMMA prepolymer prepared through the photopolymerization of MMA by the *r*-AMDV initiator, the MTEMPO mediator, and the ^tBuS photo-acid generator. The

block copolymerization continued until the reaction mixture was completely solidified. For the MMA polymerization by this system, the monomer conversion linearly increased up to 5 h, followed by a slight increase over 5 h to 10 h [41]. The GPC profiles of the prepolymer prepared by the MMA polymerization for 6.5 h and the block copolymer are shown in Figure 15. The resulting block copolymer contained the prepolymer due to the deactivation of the propagating chain end. It was found that *ca.* 75% of the prepolymer was deactivated on the basis of the area ratio of the respective molecular weights in the GPC curve of the block copolymer. The MMA polymerization was shortened to 5 h in order to prevent the deactivation of the growing chain end. As can be seen in Figure 16, the GPC curve of the block copolymer was shifted to the higher molecular weight side and contained no prepolymer. The molecular weight and its distribution of the block copolymer were estimated to be $M_n = 43,200$ and $M_w/M_n = 2.14$, while those of the prepolymer were $M_n = 10,100$ and $M_w/M_n = 1.63$. It was found that the deactivation of the propagating chain ends was caused by a decrease in the monomer concentration and occurred during the end stage of the polymerization. The absolute molecular weight of the PMMA-*b*-PⁱPMA diblock copolymer obtained by the MMA polymerization for 5 h was determined by ¹H NMR to be $M_n = 36,000$ based on the signal intensity of the methyl ester protons at 3.63 ppm and the methine protons at 4.87 ppm.

Figure 15. The GPC profiles of the resulting block copolymer (BL) and prepolymer (PR) prepared by the MMA polymerization for 6.5 h.

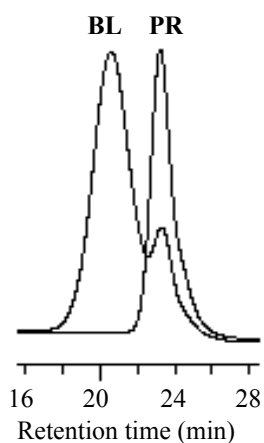
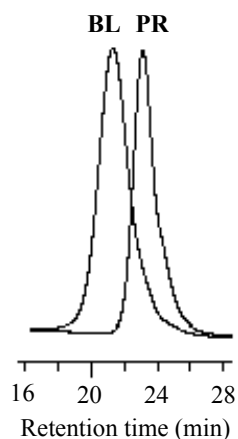


Figure 16. The GPC profiles of the resulting block copolymer (BL) and prepolymer (PR) prepared by the MMA polymerization for 5 h.



2.6. Solution Polymerization

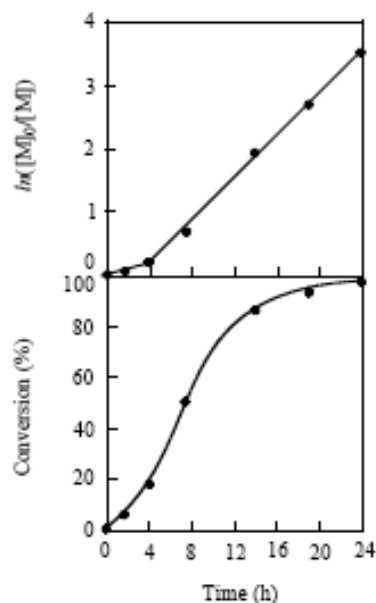
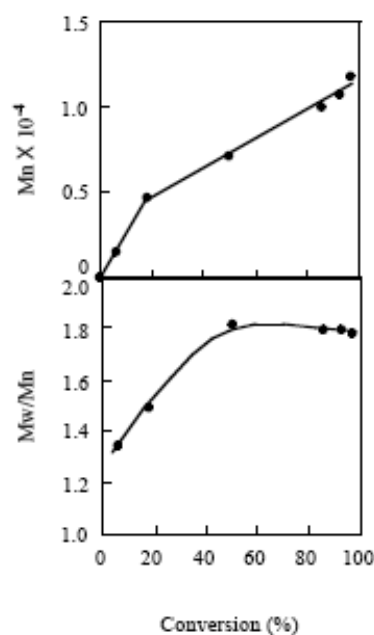
The deactivation of the growing polymer chain ends occurred during the MTEMPO-mediated photopolymerization, as well as the thermal NMP [44]. The growing polymer chain ends should be more stabilized in a solution than in the bulk, because their deactivation occurs at the end stage of the polymerization where most monomers are consumed [64,76,77], although the solution polymerization retards the propagation rate. In order to obtain more stable growing polymer chain ends, the solution polymerization was explored [45]. The polymerization was performed in acetonitrile at room temperature using the *r*-AMDV initiator and the MTEMPO mediator, and the ^tBuS photo-acid generator. The results are shown in Table 8. The solution polymerization allowed the conversion to reach 97%, whereas it was difficult for the bulk polymerization to increase the conversion over 85% [41].

Table 8. Photopolymerization of MMA in acetonitrile.

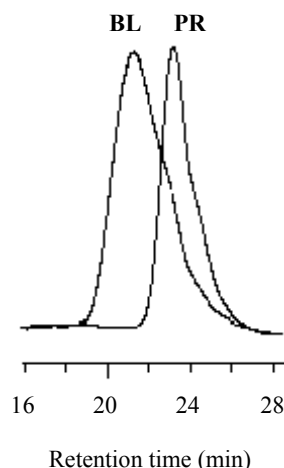
MTEMPO/ <i>r</i> -AMDV	^t BuS/MTEMPO	Conv. (%)	<i>M_n</i> ^a	<i>M_w/M_n</i> ^a
1.06	0.53	80	7,930	1.72
2.13	0.53	67	10,100	1.67
2.13	1.02	97	11,700	1.78

Irradiation time: 24 h. [MMA]₀ = 9.35 M, [MTEMPO]₀ = 0.0483 M. ^a Estimated by GPC based on PMMA standards.

The livingness of the polymerization was investigated at the MTEMPO/*r*-AMDV of 2.13 and ^tBuS/MTEMPO of 1.02. The time-conversion and its first-order plots for the polymerization are shown in Figure 17. The $\ln[M]_0/[M]$ plots showed different lines before and after 4 h, indicating that the radical concentrations were different for these two lines. The polymerization should be under the non-steady-state below 4 h and reached the steady-state over this time. The non-steady-state was not observed in the bulk polymerization [41]. It is suggested that MTEMPO could not effectively trap the propagating radical due to its low concentration in the solution polymerization, causing the occurrence of a normal termination between the propagating radicals under the non-steady-state. However, the proportion of the polymers produced by the normal termination is low based on its conversion (<18%). Figure 18 shows the plots of the molecular weight vs. the conversion for the polymerization. It was observed that oligomers with several thousand molecular weights were formed under the non-steady-state below the 18% conversion. However, the molecular weight linearly increased with the conversion under the steady-state, indicating that the polymerization proceeded by the living mechanism. The MWD was around 1.8, somewhat higher than that for the bulk polymerization. This broader MWD should be due to the presence of the oligomers produced under the non-steady-state.

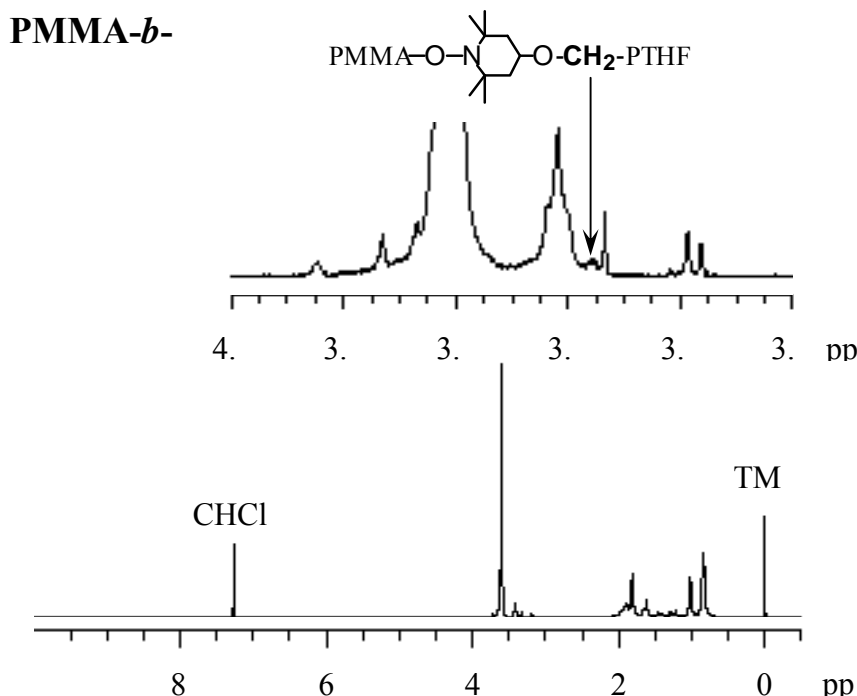
Figure 17. The time-conversion and its first order plots for the polymerization of MMA.**Figure 18.** The plots of the molecular weight and MWD vs. the conversion for the polymerization of MMA in acetonitrile. $[MMA]_0 = 9.35$ M, $MTEMPO/r\text{-AMDV} = 2.13$, $t\text{BuS}/MTEMPO = 1.02$.

The stability of the growing polymer chain ends for the solution polymerization was also investigated through the block copolymerization. The PMMA prepolymer was prepared by a 14 h polymerization. The block copolymerization was performed for 19 h using t PMA as the second monomer. Figure 19 shows the GPC profiles of the prepolymer and the block copolymer. The curve of the block copolymer was shifted to the higher molecular weight side without deactivation, indicating that the prepolymer efficiently initiated the polymerization of t PMA. The growing polymer chain ends were stabilized even at a high conversion over 85% for the solution polymerization.

Figure 19. The GPC profiles of the resulting block copolymer (BL) and prepolymer (PR).

2.7. Block Copolymerization Using a TEMPO Macromediator

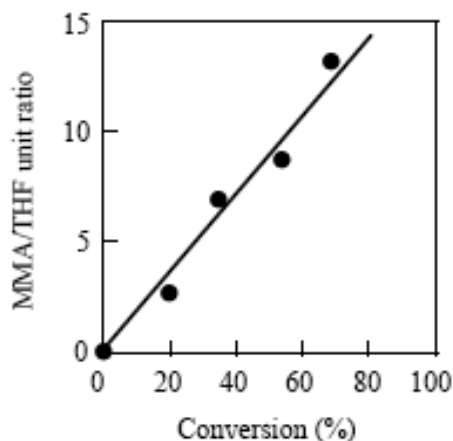
The MTEMPO-mediated photo controlled/living radical polymerization has the potential to create a variety of architectures through designing TEMPO derivatives. The synthesis of a diblock copolymer using a macromediator of TEMPO is described in this section.

Figure 20. ^1H NMR spectra of the block copolymer and the TEMPO-terminated poly(tetrahydrofuran) (PTHF-TEMPO). Solvent: CDCl_3 .

TEMPO-terminated poly(tetrahydrofuran) (PTHF-TEMPO) with $M_n = 1,720$ and $M_w/M_n = 1.91$ was used as the macromediator for the polymerization [78]. The photopolymerization of MMA was performed by AMDV, BAI, and PTHF-TEMPO [38]. Figure 20 shows the ^1H NMR spectra of the resulting block copolymer with $M_n = 11,300$ and $M_w/M_n = 1.83$. The observation of a signal of the

methylene attached to the TEMPO at 3.36 ppm confirmed that the PMMA and PTHF blocks were connected through the TEMPO. The plots of the molar ratio of the MMA unit to the THF unit *versus* the conversion using their signal intensity are shown in Figure 21. The MMA/THF ratio linearly increased with the increase in the conversion, suggesting the living nature of the polymerization.

Figure 21. The plots of molar ratio of the MMA unit to the THF unit for the copolymers *vs.* the conversion.



The living mechanism of the polymerization was also confirmed on the basis of plots of linear correlation of the molecular weight of the copolymer *vs.* the initial concentration of AMDV ($[AMDV]_0$). The MWD of the copolymers was the same as, or less than, that of PTHF-TEMPO. Linear increases in the first order time-conversion plots and the conversion-molecular weight plots endorsed the controlled/living mechanism.

2.8. Photo Dispersion Polymerization

The heterogeneous polymerization using the controlled/living radical polymerization has the potential to simultaneously control the molecular weight and particle size of a polymer. A number of the thermal controlled/living radical heterogeneous polymerization systems have been studied, and there is an outstanding review article on them [79]. The MTEMPO-mediated photo dispersion polymerization of MMA was performed at room temperature using *r*-AMDV, ^tBuS, and polyvinylpyrrolidone (PVP) as the surfactant in a mixed solvent of MeOH/water = 3/1 (v/v) [49]. Figure 22 shows SEM images of the resulting polymer particles. The photo dispersion polymerization in the absence of MTEMPO provided nonspecific particles. High molecular weight polymers should be produced by very fast uncontrolled polymerization, precipitated before being stabilized by PVP. On the other hand, the MTEMPO-mediated photo dispersion polymerization produced spherical particles of PMMA. The particle size distribution decreased as the PVP concentration increased. It was found that the size distributions were below 1.1 for the PVP concentrations of 60 and 75 wt% (Table 9). The spherical particles showed a comparatively narrow molecular weight distribution, indicating the simultaneous control of the molecular weight and particle size.

Figure 22. SEM images of the PMMA particles obtained by uncontrolled polymerization (a) without MTEMPO and t BuS; (b) without MTEMPO; and (c) without r -AMDV and MTEMPO; and the MTEMPO-mediated polymerization at different PVP concentrations: (d) 30 wt%; (e) 45 wt%; (f) 60 wt%; and (g) 75 wt%.

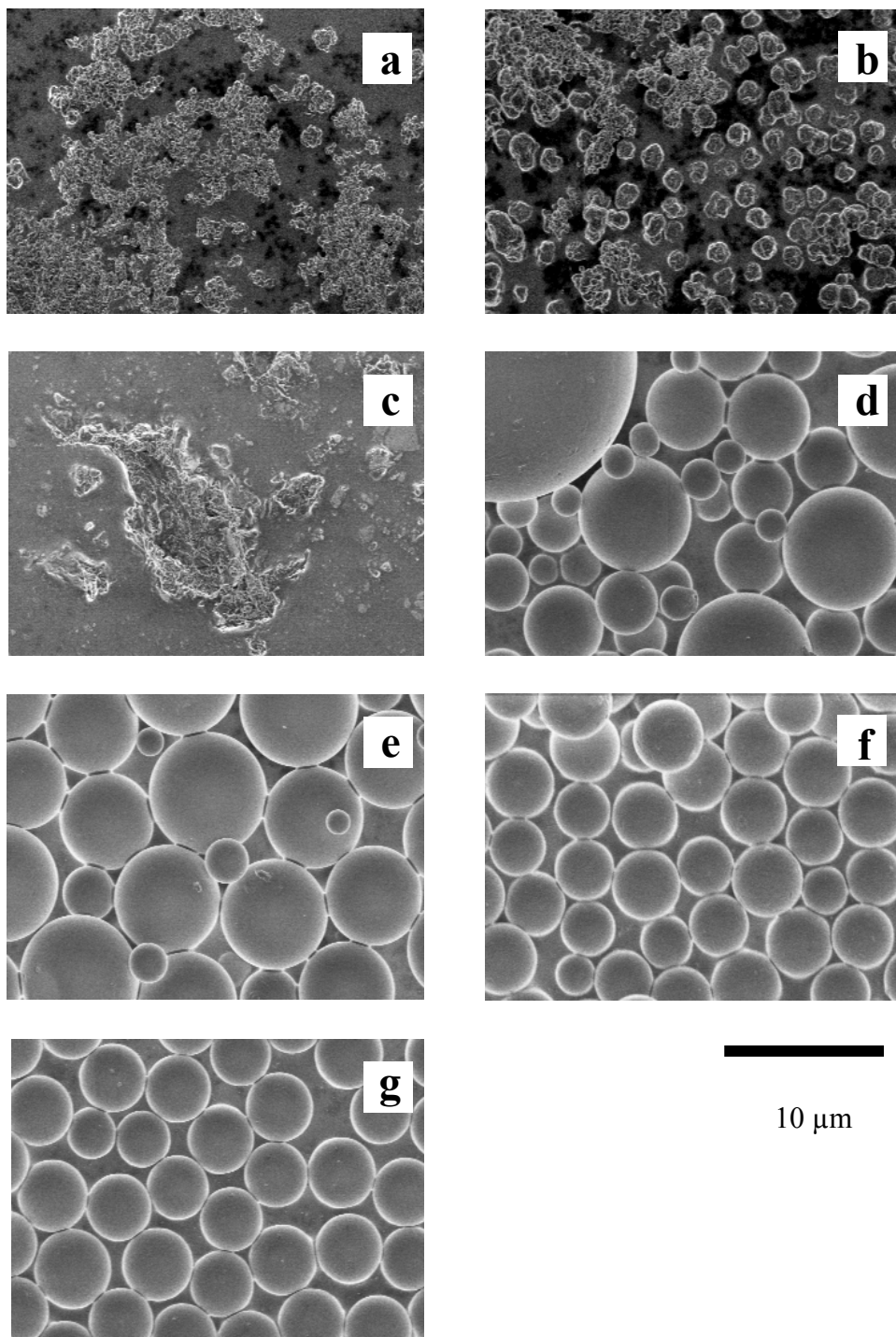


Table 9. Photo dispersion polymerization of MMA.

<i>r</i> -AMDV (μmol)	MTEMPO (μmol)	^t BuS (μmol)	PVP (wt%)	Conv. (%)	<i>Mn</i> ^a	<i>Mw/Mn</i> ^a	Morphology ^b	<i>Dn</i> ^b (μm)	<i>Dw/Dn</i> ^b
45.4	–	–	45	70	78,900	3.26	nonspecific	–	–
45.4	–	23.5	45	34	57,600	3.64	nonspecific	–	–
–	–	23.5	45	69	175,000	2.50	nonspecific	–	–
45.4	48.3	23.5	30	20	18,200	1.62	spherical	3.87	2.80
45.4	48.3	23.5	45	23	17,700	1.61	spherical	5.66	1.27
45.4	48.3	23.5	60	37	20,500	1.65	spherical	3.99	1.06
45.4	48.3	23.5	75	28	18,000	1.64	spherical	4.14	1.04

Polymerization for 6 h in the mixed solvent (MeOH/water = 3/1). ^a Estimated by GPC based on PMMA standards; ^b Determined by the SEM observation.

Figure 23. The time-conversion plots, the first order time-conversion plots, and the variation in turbidity of the polymerization system with time.

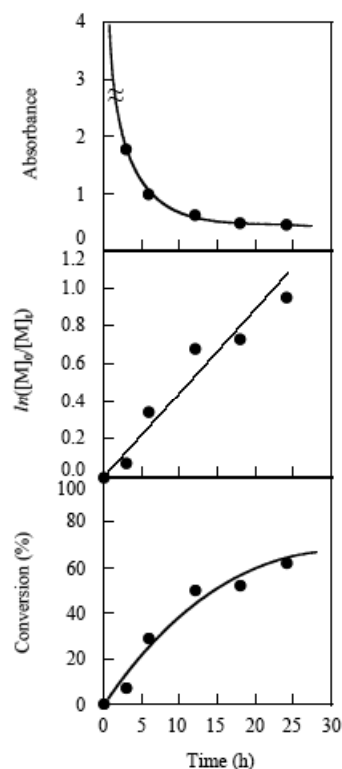


Figure 23 shows the time-conversion plots, the first order time-conversion plots, and the variation in turbidity of the polymerization system. The turbidity was determined by UV based on the absorbance at 230 nm. The turbidity of the system rapidly increased as the polymerization was initiated and became almost constant over 12 h. The constant turbidity suggests the limitation of the light passing through the system. The continued increase in the conversion in spite of the constant turbidity implies that over 12 h, the polymerization occurred outside of the particles. This inference was supported by a decrease in the molecular weight of the particles and the formation of a large amount of small particles outside of the secondary particles by the further extension of the polymerization time. The small particles had *ca.* a 1- μm diameter. It is considered that polymerization outside of the secondary

particles did not occur by the transfer of the active species in the secondary particles, but by the remaining initiator in the solution or the autopolymerization. However, polymerization outside of the secondary particles should be slow because of the low monomer concentration at the later stage of polymerization. Therefore, the simultaneous control of the molecular weight and particle size was possible as long as light penetrated into the secondary particles.

3. Conclusions

TEMPO-mediated photopolymerization is a novel method to control molecular weight by photo irradiation. This polymerization also expanded the range of applicable monomers for thermal NMP, because photopolymerization has already been applied to other vinyl monomers, such as vinyl acetate [40] and ethyl acrylate [48]. This TEMPO-mediated controlled/living photoradical polymerization should expand the scope of molecular design and its industrial applications.

4. Experimental Section

Instrumentation The photopolymerization was carried out using a Wacom HX-500 illuminator with a 500 W high-pressure mercury lamp and an Ushio optical modulex BA-H502, an illuminator OPM2-502H with a high-illumination lens UI-OP2SL, and a 500 W super high-pressure UV lamp (USH-500SC2, Ushio Co. Ltd.). Gel permeation chromatography (GPC) was performed using a Tosoh GPC-8020 instrument equipped with a DP-8020 dual pump, a CO-8020 column oven, and a RI-8020 refractometer. Three polystyrene gel columns, Tosoh TSKGEL G2000H_{XL}, G4000H_{XL}, and G6000H_{XL} were used with THF as the eluent at 40 °C. UV spectra were obtained using a Shimadzu UV-160A UV-Vis recording spectrophotometer. Gas chromatography (GC) was performed with Shimadzu GC-8A. Differential scanning calorimetry (DSC) was performed by a Shimadzu DSC-60 instrument equipped with a TA-60WS system controller and a FC-60 nitrogen flow controller. Scanning electron microscopy (SEM) measurements were performed using a Hitachi SU8000 scanning electron microscope. Centrifugation of polymer particles was carried out using a Tomy LC-200 centrifugal separator.

Materials All the azoinitiators were purified by recrystallization in methanol. Racemic-(2RS,2'RS)-azobis(4-methoxy-2,4-dimethylvaleronitrile) (*r*-AMDV) and meso-(2RS,2'SR)-azobis(4-methoxy-2,4-dimethylvaleronitrile) (*m*-AMDV) were obtained by separation from their mixture by recrystallization from ether [67]. 4-Methoxy-TEMPO was prepared as reported previously [80]. All the photo-acid generators were used as received. MMA and ¹PMA were washed with 5 wt% sodium hydroxide solution and water and then distilled over calcium hydride. PTHF-TEMPO was prepared as reported previously [78]. PVP (K30) with the average molecular weight of Mw ≈ 40,000 was purchased from Wako Pure Chemicals Co. Ltd and was used without further purification.

Photopolymerization General Procedure MMA (936 mg, 9.35 mmol), *r*-AMDV (14 mg, 0.0454 mmol), MTEMPO (9 mg, 0.0483 mmol), and ¹BuS (11 mg, 0.0341 mmol) were placed in an ampoule. After degassing the contents, the ampoule was sealed under vacuum. The bulk polymerization was carried out at room temperature for 9.5 h with irradiation by reflective light using a mirror with a 500W high-pressure mercury lamp at 7.0 Å. The resulting mass was dissolved in dichloromethane (10 mL). The solution was concentrated by an evaporator to remove the dichloromethane and the monomer unreacted and was freeze-dried with benzene (30 mL) at 40 °C to

obtain the product as white powder (664 mg). The conversion was estimated with the weight. The product was dissolved in dichloromethane (5 mL) and poured into hexane (500 mL). The precipitate was collected by filtration and dried *in vacuo* for several hours to be subjected to GPC analysis.

Photopolymerization of MMA by PTHF-TEMPO: General Procedure A mixture of MMA (936 mg, 9.35 mmol), PTHF-TEMPO (24 mg, 0.0240 mmol as the TEMPO content), AMDV (7 mg, 0.0227 mmol), and BAI in 50 wt% propylene carbonate solution (19 mg, 0.0125 mmol) was placed in an ampoule. After degassing the contents, the ampoule was sealed under vacuum. The polymerization was carried out at room temperature for 6 h with irradiation by reflective light using a mirror with a 500 W high-pressure mercury lamp at 7.0 Å. The resulting mixture was dissolved in dichloromethane (10 mL). Ethylbenzene was added as a standard to the dichloromethane solution, and the solution was subjected to GC. The solution was concentrated to 3 mL with an evaporator and was poured into hexane (500 mL) to remove the monomer and PTHF-TEMPO unreacted. The precipitate was collected by filtration and dried *in vacuo* for several hours. The resulting polymer was freeze-dried with benzene to obtain the PMMA-*b*-PTHF (472 mg, 50% in yield).

Dispersion polymerization: General procedure MMA (936 mg, 9.35 mmol), *r*-AMDV (14 mg, 0.0454 mmol), MTEMPO (9 mg, 0.0483 mmol), ^tBuS (11 mg, 0.0235 mmol), PVP (421.6 mg, 45 wt% to MMA), MeOH (7.5 mL), and water (2.5 mL) were placed in an ampoule. After degassing the contents, the ampoule was sealed under vacuum. The polymerization was carried out at room temperature at 400 rpm for 12 h with irradiation by reflective light using a mirror with the high-pressure UV lamp. The resulting particles of PMMA were cleaned with MeOH by a repeated sedimentation-redispersion process. The conversion was estimated gravimetrically. The polymer particles were dried *in vacuo* for several hours and were obtained as white powder (465 mg).

References

1. Odian, G. Radical chain polymerization. In *Principles of Polymerization*, 4th ed.; John Wiley & Sons, Inc.: Hoboken, NJ, USA, 2004.
2. Otsu, T. Organic polysulfides as polymerization initiators. *J. Polym. Sci.* **1956**, *21*, 559–561.
3. Moad, G.; Rizzardo, E.; Thang, S.H. Toward living radical polymerization. *Accounts Chem. Res.* **2008**, *41*, 1133–1142.
4. Braunecker, W.A.; Matyjaszewski, K. Controlled/living radical polymerization: Features, developments, and perspectives. *Prog. Polym. Sci.* **2007**, *32*, 93–146.
5. Uegaki, H.; Kotani, Y.; Kamigaito, M.; Sawamoto, M. Nickel-mediated living radical polymerization of methyl methacrylate. *Macromolecules* **1997**, *30*, 2249–2253.
6. Wayland, B.B.; Poszmik, G.; Mukerjee, S.L. Living radical polymerization of acrylates by organocobalt porphyrin complexes. *J. Am. Chem. Soc.* **1994**, *116*, 7943–7944.
7. Ando, T.; Kamigaito, M.; Sawamoto, M.; Higashimura, T. Iron(II) chloride complex for living radical polymerization of methyl methacrylate. *Macromolecules* **1995**, *30*, 4507–4510.
8. Kato, M.; Kamigaito, M.; Sawamoto, M.; Higashimura, T. Polymerization of methyl methacrylate with the carbon tetrachloride/dichlorotris-(triphenylphosphine)ruthenium(II)/methylaluminum bis(2,6-di-*tert*-butylphenoxide) initiating system: Possibility of living radical polymerization. *Macromolecules* **1995**, *28*, 1721–1723.

9. Percec, V.; Barboiu, B.; Neumann, A.; Ronda, J.C.; Zhao, M. Metal-catalyzed “living” radical polymerization of styrene initiated with arenesulfonyl chlorides. From heterogeneous to homogeneous catalysis. *Macromolecules* **1996**, *29*, 3665–3668.
10. Lecmote, P.; Drapier, I.; Dubois, P.; Teyssie, P.; Jerome, R. Controlled radical polymerization of methyl methacrylate in the presence of palladium acetate, triphenylphosphine, and carbon tetrachloride. *Macromolecules* **1997**, *30*, 7631–7633.
11. Kotani, Y.; Kamigaito, M.; Sawamoto, M. Re(V)-mediated living radical polymerization of styrene: $\text{ReO}_2\text{I}(\text{PPh}_3)_2/\text{R-I}$ initiating systems. *Macromolecules* **1999**, *32*, 2420–2424.
12. Oka, M.; Tatemoto, M. Vinylidene fluoride–Hexafluoropropylene copolymer having terminal iodines. In *Contemporary Topics in Polymer Science*; Plenum Press: New York, NY, USA, 1984.
13. Lacroix-Desmazes, P.; Severac, R.; Boutevin, B. Reverse iodine transfer polymerization of methyl acrylate and *n*-butyl acrylate. *Macromolecules* **2005**, *38*, 6299–6309.
14. Pouget, E.; Tonnar, J.; Eloy, C.; Lacroix-Desmazes, P.; Boutevin, B. Synthesis of poly(styrene)-*b*-poly(dimethylsiloxane)-*b*-poly(styrene) triblock copolymers by iodine transfer polymerization in miniemulsion. *Macromolecules* **2006**, *39*, 6009–6016.
15. Hawker, C.J.; Bosman, A.W.; Harth, E. New polymer synthesis by nitroxide mediated living radical polymerizations. *Chem. Rev.* **2001**, *101*, 3661–3688.
16. Sciannamea, V.; Jérôme, R.; Detrembleur, C. *In situ* nitroxide-mediated radical polymerization (NMP) processes: Their understanding and optimization. *Chem. Rev.* **2008**, *108*, 1104–1126.
17. Yousi, Z.; Jian, L.; Rongchuan, Z.; Jianliang, Y.; Lizong, D.; Lansun, Z. Synthesis of block copolymer from dissimilar vinyl monomer by stable free radical polymerization. *Macromolecules* **2000**, *33*, 4745–4749.
18. Devonport, W.; Michalak, L.; Malmstrom, E.; Mate, M.; Kurdi, B.; Hawker, C.J.; Barclay, G.G.; Sinta, R. “Living” free-radical pin the absence of initiators: Controlled autopolymerization. *Macromolecules* **1997**, *30*, 1929–1934.
19. Mardare, D.; Matyjaszewski, K. “Living” radical polymerization of vinyl acetate. *Macromolecules* **1994**, *27*, 645–649.
20. Granel, C.; Jerime, R.; Teyssie, P.; Jasieczek, C.B.; Shooter, A.J.; Haddleton, D.M.; Hastings, J.J.; Gigmes, D.; Grimaldi, S.; Tordo, P.; Greszta, D.; Matyjaszewski, K. Investigation of methyl methacrylate and vinyl acetate polymerization promoted by $\text{Al}(\text{tBu})_3/2,2'$ -bipyridine and $\text{Al}(\text{tBu})_3/2,2'$ -bipyridine/TEMPO complexes. *Macromolecules* **1998**, *31*, 7133–7141.
21. Matyjaszewski, K.; Gaynor, S.; Greszta, D.; Mardare, D.; Shigemoto, T. “Living” and controlled radical polymerization. *J. Phys. Org. Chem.* **1995**, *8*, 306–315.
22. Hawker, C.J.; Barclay, G.G.; Orellana, A.; Dao, J.; Devonport, W. Initiating systems for nitroxide-mediated “living” free radical polymerizations: Synthesis and evaluation. *Macromolecules* **1996**, *29*, 5245–5254.
23. Dao, J.; Benoit, D.; Hawker, C.J. A versatile and efficient synthesis of alkoxyamine LFR initiators via manganese based asymmetric epoxidation catalysts. *J. Polym. Sci. A Polym. Chem.* **1998**, *36*, 2161–2167.
24. Benoit, D.; Chaplinski, V.; Braslau, R.; Hawker, C.J. Development of a universal alkoxyamine for “living” free radical polymerizations. *J. Am. Chem. Soc.* **1999**, *121*, 3904–3920.

25. Veregin, R.P.N.; Georges, M.K.; Hamer, G.K.; Kazmaier, P.M. mechanism of living free radical polymerizations with narrow polydispersity: Electron spin resonance and kinetic studies. *Macromolecules* **1995**, *28*, 4391–4398.
26. Greszta, D.; Matyjaszewski, K. Comments on the paper “living radical polymerization: Kinetic results”. *Macromolecules* **1996**, *29*, 5239–5240.
27. Braslau, R.; Burrill, II, L.C.; Siano, M.; Naik, N.; Howden, R.K.; Mahal, L.K. Low-temperature preparations of unimolecular nitroxide initiators for “living” free radical polymerizations. *Macromolecules* **1997**, *30*, 6445–6450.
28. Li, I.Q.; Howell, B.A.; Koster, R.A.; Priddy, D.B. Mono- and dinitroxide styrene polymerization initiators. *Macromolecules* **1996**, *29*, 8554–8555.
29. Mercier, C.L.; Acerbis, S.; Bertin, D.; Chauvin, F.; Gimes, D.; Guerret, O.; Lansalot, M.; Marque, S.; Moigne, F.L.; Fischer, H.; Tordo, P. Design and use of β -phosphorus nitroxides and alkoxyamines in controlled/“living” free radical polymerizations. *Macromol. Symposia* **2002**, *182*, 225–247.
30. Yoshida, E.; Ishizone, T.; Hirao, A.; Nakahama, S.; Takata, T.; Endo, T. Synthesis of polystyrene having an aminoxy terminal by the reactions of living polystyrene with an oxoammonium salt and with the corresponding nitroxyl radical. *Macromolecules* **1994**, *27*, 3119–3124.
31. Yoshida, E.; Nakamura, K.; Takata, T.; Endo, T. Oxoammonium salts as initiators for cationic polymerization of vinyl monomers. *J. Polym. Sci. A Polym. Chem.* **1993**, *31*, 1505–1512.
32. Pyun, J.; Tang, C.; Kowalewski, T.; Fréchet, J.M.J.; Hawker, C.J. Synthesis and direct visualization of block copolymers composed of different macromolecular architectures. *Macromolecules* **2005**, *38*, 2674–2685.
33. Hawker, C.J.; Hedrick, J.L. Accurate control of chain ends by a novel “living” free-radical polymerization process. *Macromolecules* **1995**, *28*, 2993–2995.
34. Hawker, C.J. Architectural Control in “Living” free radical polymerizations: Preparation of star and graft polymers. *Angew. Chem. Int. Ed. Eng.* **1995**, *134*, 1456–1459.
35. Tsoukatos, T.; Pispas, S.; Hadjichristidis, N. Complex macromolecular architectures by combining TEMPO living free radical and anionic polymerization. *Macromolecules* **2000**, *33*, 9504–9511.
36. Yoshida, E. Photo-living radical polymerization of methyl methacrylate by a nitroxide mediator. *Colloid Polym. Sci.* **2008**, *286*, 1663–1666.
37. Yoshida, E. Photo-living radical polymerization of methyl methacrylate by 2,2,6,6-tetramethylpiperidine-1-oxyl in the presence of a photo-acid generator. *Colloid Polym. Sci.* **2009**, *287*, 767–772.
38. Yoshida, E. Synthesis of poly(methyl methacrylate)-*block*-poly(tetrahydrofuran) by photo-living radical polymerization using a 2,2,6,6-tetramethylpiperidine-1-oxyl macromediator. *Colloid Polym. Sci.* **2009**, *287*, 1417–1424.
39. Yoshida, E. Photo-living radical polymerization of methyl methacrylate using alkoxyamine as an initiator. *Colloid Polym. Sci.* **2010**, *288*, 7–13.
40. Yoshida, E. Nitroxide-mediated photo-living radical polymerization of vinyl acetate. *Colloid Polym. Sci.* **2010**, *288*, 73–78.

41. Yoshida, E. Nitroxide-mediated photo-living radical polymerization of methyl methacrylate using (4-*tert*-butylphenyl)diphenylsulfonium triflate as a photo-acid generator. *Colloid Polym. Sci.* **2010**, *288*, 239–243.
42. Yoshida, E. Effect of azoinitiators on nitroxide-mediated photo-living radical polymerization of methyl methacrylate. *Colloid Polym. Sci.* **2010**, *288*, 341–345.
43. Yoshida, E. Effects of initiators and photo-acid generators on nitroxide-mediated photo-living radical polymerization of methyl methacrylate. *Colloid Polym. Sci.* **2010**, *288*, 901–905.
44. Yoshida, E. Stability of growing polymer chain ends for nitroxide-mediated photo-living radical polymerization. *Colloid Polym. Sci.* **2010**, *288*, 1027–1030.
45. Yoshida, E. Nitroxide-mediated photo-living radical polymerization of methyl methacrylate in solution. *Colloid Polym. Sci.* **2010**, *288*, 1639–1643.
46. Yoshida, E. Nitroxide-mediated photo-living radical polymerization of methyl methacrylate in the presence of (η^6 -benzene)(η^5 -cyclopentadienyl)Fe^{II} hexafluorophosphate. *Colloid Polym. Sci.* **2010**, *288*, 1745–1749.
47. Yoshida, E. Graft copolymerization of methyl methacrylate on polystyrene backbone through nitroxide-mediated photo-living radical polymerization. *Colloid Polym. Sci.* **2011**, *289*, 837–841.
48. Yoshida, E. Nitroxide-mediated photo-controlled/living radical polymerization of ethyl acrylate. *Colloid Polym. Sci.* **2011**, *289*, 1127–1132.
49. Yoshida, E. Nitroxide-mediated photo-controlled/living radical dispersion polymerization of methyl methacrylate. *Colloid Polym. Sci.* **2011**, *289*, 1625–1630.
50. Guillaenuef, Y.; Bertin, D.; Gimes, D.; Versace, D.; Lalevee, J.; Fouassier, J. Toward nitroxide-mediated photopolymerization. *Macromolecules* **2010**, *43*, 2204–2212.
51. Goto, A.; Scaiano, J.C.; Maretti, L. Photolysis of an alkoxyamine using intramolecular energy transfer from a quinoline antenna — Towards photo-induced living radical polymerization. *Photochem. Photobiol. Sci.* **2007**, *6*, 833–853.
52. Lalevee, J.; Allonas, X.; Fouassier, J.P. A new efficient photoiniferter for living radical photopolymerization. *Macromolecules* **2006**, *39*, 8216–8218.
53. Nemoto, Y.; Nakayama, Y. Optimal irradiation wavelength in iniferter-based photocontrolled radical polymerization. *J Polym. Sci. A Polym. Chem.* **2008**, *46*, 4505–4512.
54. You, Y.; Hong, C.; Bai, R.; Pan, C.; Wang, J. Photo-initiated living free radical polymerization in the presence of dibenzyl trithiocarbonate. *Macromol. Chem. Phys.* **2002**, *203*, 477–483.
55. Ran, R.; Yu, Y.; Wan, T. Photoinitiated RAFT polymerization in the presence of trithiocarbonate. *J. Appl. Polym. Sci.* **2007**, *105*, 398–404.
56. Baruah, S.R.; Kakati, D.K. Photopolymerization of methyl methacrylate by 2,2'-dithiodiethanol: Effect of reaction conditions. *J. Appl. Polym. Sci.* **2006**, *100*, 1601–1606.
57. Ajayaghosh, A.; Francis, R.A. A xanthate-derived photoinitiator that recognizes and controls the free radical polymerization pathways of methyl methacrylate and styrene. *J. Am. Chem. Soc.* **1999**, *121*, 6599–6606.
58. Yang, W.; Ranby, B. Radical living graft polymerization on the surface of polymeric materials. *Macromolecules* **1996**, *29*, 3308–3310.

59. Tasdelen, M.A.; Durmaz, Y.Y.; Karagoz, B.; Bicak, N.; Yagci, Y. A new photoiniferter/RAFT agent for ambient temperature rapid and well-controlled radical polymerization. *J. Polym. Sci. A Polym. Chem.* **2008**, *46*, 3387–3395.
60. Ajayaghosh, A.; Francis, R. Narrow polydispersed reactive polymers by a photoinitiated free radical polymerization approach. Controlled polymerization of methyl methacrylate. *Macromolecules* **1998**, *31*, 1436–1438.
61. Yin, H.; Zheng, H.; Lu, L.; Liu, P.; Cai, Y. Highly efficient and well-controlled ambient temperature RAFT polymerization of glycidyl methacrylate under visible light radiation. *J. Polym. Sci. A Polym. Chem.* **2007**, *45*, 5091–5102.
62. Cohen, N.A.; Tillman, E.S.; Thakur, S.; Smith, J.R.; Eckenhoff, W.T.; Pintauer, T. Effect of the ligand in atom transfer radical polymerization reactions initiated by photodimers of 9-bromoanthracene. *Macromol. Chem. Phys.* **2009**, *210*, 263–268.
63. Li, P.; Qiu, K. Cu(S₂CNEt₂)Cl-catalyzed reverse atom-transfer radical polymerization of vinyl monomers. *Macromol. Rapid Commun.* **2002**, *23*, 1124–1129.
64. Yoshida, E.; Okada, Y. Living radical polymerization of styrene in the presence of 4-hydroxy-2,2,6,6-tetramethylpiperidine-1-oxyl, and radical transformation of the resulting polymers by other radicals. *Bull. Chem. Soc. Jpn.* **1997**, *70*, 275–281.
65. McHale, R.; Aldabbagh, F.; Zetterlund, P.B. The role of excess nitroxide in the SG1 (*N*-tert-butyl-*N*-[1-diethylphosphono-(2,2-dimethylpropyl)] nitroxide)-mediated polymerization of methyl methacrylate. *J. Polym. Sci. A Polym. Chem.* **1999**, *45*, 2194–2203.
66. Bovey, F.A.; Tiers, G.V.D. Polymer NSR spectroscopy. II. The high resolution spectra of methyl methacrylate polymers prepared with free radical and anionic initiators. *J. Polym. Sci.* **1960**, *44*, 173–182.
67. Kita, Y.; Gotanda, K.; Murata, K.; Suemura, M.; Sano, A.; Yamaguchi, T.; Oka, M.; Matsugi, M. Practical radical additions under mild conditions using 2,2'-azobis(2,4-dimethyl-4-methoxyvaleronitrile) [V-70] as an initiator. *Org. Process Res. Dev.* **1998**, *2*, 250–254.
68. Crivello, J.V.; Sangermano, M. Visible and long-wavelength photoinitiated cationic polymerization. *J. Polym. Sci. A Polym. Chem.* **2001**, *39*, 343–356.
69. Crivello, J.V. The discovery and development of onium salt cationic photoinitiators. *J. Polym. Sci. A Polym. Chem.* **1999**, *37*, 4241–4254.
70. Devoe, R.J.; Sahyunn, M.R.V.; Sepone, D.; Sharmac, D.K. Transient intermediates in the photolysis of iodonium cations. *Can. J. Chem.* **1987**, *65*, 2342–2349.
71. Crivello, J.V.; Lam, J.H. W.; Moore, J.E.; Schroeter, S.H. Triarylsulfonium salts: A new class of photoinitiators for cationic polymerization. *J. Radiat. Curing* **1978**, *5*, 2–17.
72. Crivello, J.V.; Lam, J.H.W. Complex triarylsulfonium salt photoinitiators. I. The identification, characterization, and syntheses of a new class of triarylsulfonium salt photoinitiators. *J. Polym. Sci. Polym. Chem. Ed.* **1980**, *18*, 2677–2695.
73. Crivello, J.V.; Lam, J.H.W. Photoinitiated cationic polymerization with triarylsulfonium salts. *J. Polym. Sci. Polym. Chem. Ed.* **1979**, *17*, 977–999.
74. Liu, Y.C.; Wu, L.M.; Chen, P.A. Facile generation of radical cations via the action of nitroxides. *Tetrahedron Lett.* **1985**, *26*, 4201–4202.

75. Meier, K.; Zweifel, H. Photoinitiated cationic polymerization of epoxides with iron-arene complexes. *J. Radiat. Curing* **1986**, *13*, 26–32.
76. Li, I., Howell, B.A., Matyjaszewski, K., Shigemoto, T., Smith, P.B.; Priddy, D.B. Kinetics of decomposition of 2,2,6,6-tetramethyl-1-(1-phenylethoxy)piperidine and its implications on nitroxyl-mediated styrene polymerization. *Macromolecules* **1995**, *28*, 6692–6693.
77. Yoshida, E.; Sugita, A. Synthesis of poly(styrene-*b*-tetrahydrofuran-*b*-styrene) triblock copolymers by transformation from living cationic into living radical polymerization using 4-hydroxy-2,2,6,6-tetramethylpiperidine-1-oxyl as a transforming agent. *J. Polym. Sci. Polym. Chem. Ed.* **1998**, *36*, 2059–2068.
78. Yoshida, E.; Sugita, A. Synthesis of poly(tetrahydrofuran) with a nitroxyl radical at the chain end, and its application to living radical polymerization. *Macromolecules* **1996**, *29*, 6422–6426.
79. Zetterlund, P.B.; Kagawa, Y.; Okubo, M. Controlled/living radical polymerization in dispersed systems. *Chem. Rev.* **2008**, *108*, 3747–3794.
80. Miyazawa, T.; Endo, T.; Shiihashi, S.; Ogawara, M. Selective oxidation of alcohols by oxoamminium salts (R₂N:O⁺ X⁻). *J. Org. Chem.* **1985**, *50*, 1332–1334.

© 2012 by the authors; licensee MDPI, Basel, Switzerland. This article is an open access article distributed under the terms and conditions of the Creative Commons Attribution license (<http://creativecommons.org/licenses/by/3.0/>).